

Co-optimization of a piezoelectric energy harvesting system for broadband operation

S Zhao¹, U Radhakrishna², S Hanly³, J Ma⁴, J H Lang² and D Buss⁵

¹ School of Microelectronics, Tianjin University, Tianjin 300072, China

² Department of Electrical Engineering & Computer Science, Massachusetts Institute of Technology, Cambridge, MA 02139, USA

³ Mide Technology, Medford, MA 02155, USA

⁴ School of Computers, Guangdong University of Technology, Guangzhou 510006, China

⁵ Texas Instruments, Dallas, Texas 75243, USA

E-mail: shengzhao@tju.edu.cn

Abstract. The goal of this research is to increase the bandwidth (BW) over which substantial energy can be harvested using a piezoelectric energy harvester (PEH). The key innovation is the use of bias-flip (BF) electronics at the output of a PEH having a large electromechanical coupling coefficient κ_e^2 . For a PEH with large κ_e^2 , the open-circuit resonance frequency f_{oc} is substantially larger than the short-circuit resonance frequency f_{sc} . Over the intervening range, the reactive part of the conjugate matched load impedance is small, and can be approximated using BF electronics in which the BF voltage is sufficiently small and the BF losses are small. This results in a large BW over which substantial energy can be harvested. Experimental results using a commercially available PEH are presented to demonstrate this concept. Design guidelines are provided for achieving PEHs having increased κ_e^2 .

1. Introduction

Kinetic energy harvesters have become a viable source of electric power for low-power wireless sensor networks that might be connected to the Internet of Things. Of the many harvesters through which kinetic energy can be converted to electric energy, PEHs are often favored for their simple structure, their high power density, their high output voltage, and their ease of self starting. However, for the common low-loss resonant PEHs, the harvested power drops off dramatically when the ambient vibration frequency deviates from the resonance frequency of the PEH; only at the resonant frequency can the PEH output maximum power. This is problematic when PEH manufacturing tolerances and/or uncertainties in the vibration spectrum result in a frequency mismatch. In such cases it is desirable to increase the energy harvesting BW.

Several nonlinear interface circuits such as SSHI, BF, SECE and SSDCI have been proposed to increase the harvested power [1-5]. These techniques were demonstrated to be efficient at the resonance frequency of the PEH. At frequencies away from resonance, it was subsequently shown that BF employing universal phase can effectively optimize output power [6]. The BF technique shares features that are common with the independently developed P-SSHI- ϕ technique [7]. Even so, for a PEH with a small coupling coefficient (κ_e^2), the BF losses limit output power away from resonance because the BF voltage for frequencies away from resonance becomes large. Therefore, to compensate for the limited output power, this paper studies the resonance splitting behaviour

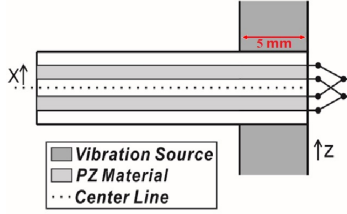


Figure 1. Schematic of a cantilever PEH.

of PEHs with large κ_e^2 , which was initially explored in [8] with only resistive load. Resonance splitting with large κ_e^2 gives two well-separated output power peaks between which (and slightly beyond) BF electronics can harvest near peak power, thereby extending the harvesting BW. With a combination of BF employing universal phase, and a PEH having large κ_e^2 , the energy harvesting BW can be further increased. Experimental results with a commercially-available PEH having $\kappa_e^2=0.069$ are presented to demonstrate this concept. With the help of BF, a peak power of $112 \mu\text{W}$, and a 3-dB BW of 50 Hz over which substantial energy is harvested, are achieved. Additionally, this paper provides design guidelines for achieving PEHs having larger κ_e^2 , and a new PEH is suggested to improve the BW performance of the existing commercial PEH.

2. Characterization of a Commercial PEH

The energy harvesting approach proposed here is studied experimentally with a commercial PEH. Mide PPA2014 PEH was selected because of its large κ_e^2 . Figure 1 shows a cross section of this cantilever device. Figure 2a shows the equivalent circuit for the PEH that defines the compact model (CM) parameters. Extracted CM parameters and output voltage measurements made using 1-g acceleration and a 5 mm clamping overlap are shown in Figure 2b. Four frequencies are important to understand power output from a cantilevered PEH. They are explained in Table 1. The matched-load (ML) resistance R_{ML} gives maximum output power at the lower zero-Thevenin-reactance frequency f_{ZR1} .

At the two frequencies f_{ZR1} and f_{ZR2} , the reactive part of the impedance looking into the output terminals of the circuit model in Figure 2a is zero. At these frequencies the source force (voltage V_F) and velocity (current I_S) are in phase, and maximum power is delivered to a resistive load that is matched to the internal resistance of the device.

3. Bias-Flip Circuit

Figure 2c shows the DC rectification and storage (DCRS) circuit used here. The BF inductor, shown in the shaded area, is used to implement the tunable inductive or capacitive reactive impedance that is required to deliver maximum output power to the storage cell at a given vibration frequency. Operation of the BF or switched inductor has been described in detail elsewhere [1-3], and used in a variety of ways to increase output power from a PEH [4, 5]. Here, the bias, that is V_{Out} across C_P , is flipped so as to produce a waveform having a phase $\phi(V_{Opt})$ in Figure 2d that would result if a matched reactive load were used in place of the BF inductor.

The BF timing is determined as follows. Begin with the AC Matched Load (ACML) circuit shown in Figure 2d. At each vibration frequency, the conjugate-matched impedance that delivers maximum real power to the matched resistive load is determined. With this impedance the phase $\phi(f)$ of the voltage V_{Out} relative to the source voltage V_F is determined to be

$$\phi(f) = \tan^{-1} [(1/(2\pi f C_m) - 2\pi f L_m)/R_m] \quad (1)$$

The bias-flipped voltage V_{Out} is then flipped at the phase $\phi(f)$ relative to V_F . Despite the

Table 1. Four frequencies that are important to understanding a cantilever PEH.

Value (Hz)	Definition
$f_{sc}=673.00$	short-circuit resonance frequency
$f_{ZR1}=673.43$	lower zero Thevenin reactance frequency
$f_{ZR2}=695.72$	upper zero Thevenin reactance frequency
$f_{oc}=696.00$	open circuit resonance frequency

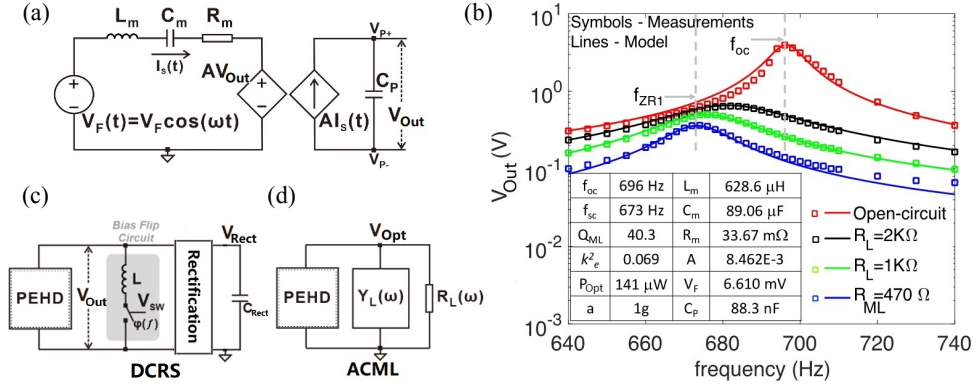


Figure 2. (a) Equivalent circuit of a PEH, (b) CM parameters, simulated and measured voltage curves of the Mide PPA2014 PEH for various resistive loads with a 5 mm clamping overlap, (c) DCRS circuit and (d) ACML circuit.

BF timing, to achieve maximum output power, in ACML case the matched resistive load R_L is required, while for DCRS case an optimum rectification voltage V_{Rect} is required.

It is well-known that the maximum output power from a PEH is given by

$$P_{Opt} = m^2 a^2 / (8\eta) = V_F^2 / (8R_m) \quad (2)$$

For the ACML circuit, this maximum output power is achieved at all frequencies. The black dashed curve of Figure 4a shows that, if the conjugate matched reactive load is replaced by a BF circuit having 100% BF efficiency (no inductor loss), and the resistive load is replaced by an ideal rectifier having the proper V_{Rect} , the power delivered to the storage cell is within 5% of P_{Opt} over a wide frequency range. As will be seen in Figure 3, the V_{Out} waveform in the BF/DCRS circuit looks very different from the sinusoidal voltage in the ACML circuit. In spite of this, ACML output power is a good predictor for BF/DCRS output power.

A limitation of the BF technique is that its efficiency is typically between 80% and 90% [6]; the losses occur in the inductor and switch. When a PEH with low κ_e^2 is used, the BF voltage for frequencies away from resonance becomes large, and BF losses limit output power [3, 7]. However, for PEHs having large κ_e^2 , f_{sc} and f_{oc} become well separated, the BF voltage in this range becomes low, and BF losses become small, thereby increasing the BW over which substantial energy can be harvested. The low BF voltage in this range is illustrated by the simulations in Figure 3. This behavior can be understood by analogy to the ACML circuit. For each vibration frequency f , there is a matched load resistor that gives optimum output power, and this resistor defines a resonance frequency f_{res} . Between BF pulses, the voltage oscillates at f_{res} . For the region between f_{sc} and f_{oc} , f_{res} is close to the vibration frequency f . Because of this, a very small tweak is required by the BF circuit to achieve the correct phase of V_{Out} . Far above f_{oc} and far below f_{sc} , there is a large difference between f_{res} and f , and a large BF voltage is required. In summary, the combination of BF and large κ_e^2 can be used to significantly extend the range over which a PEH can produce (near) maximum power output without the need for high-voltage loading electronics.

4. Experimental and Simulation Results

To demonstrate widening of the frequency range over which (near) maximum power can be harvested, experiments and simulations are performed with the Mide PPA2014 PEH described in Section 2. A 1-g acceleration and a 5 mm clamping overlap are used. The results shown in Figure 4 are based on the DCRS circuit shown in Figure 2c in which the rectifier is a diode

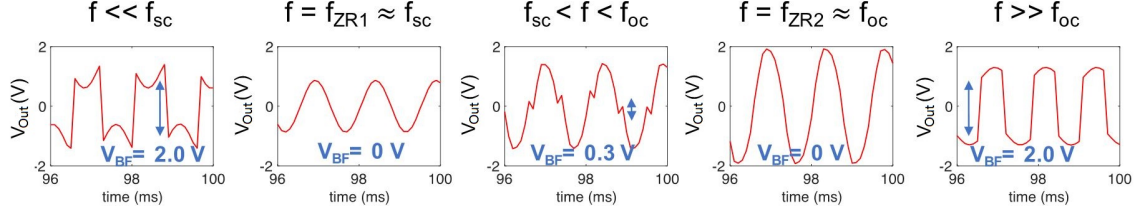


Figure 3. Waveforms of V_{Out} for selected vibration frequencies. For $f \ll f_{sc}$ and $f \gg f_{oc}$, the BF voltage V_{BF} is large, and BF loss is significant. However, for $f_{sc} < f < f_{oc}$ V_{BF} is small. At the two zero-Thevenin reactance frequencies $f_{ZR1} \approx f_{sc}$ and at $f_{ZR2} \approx f_{oc}$, $V_{BF} = 0V$.

bridge. Output power is optimized by varying V_{Rect} at each frequency. The blue curve shows that, even with 82% BF efficiency, the output power is very near the theoretical maximum (green curve) between f_{sc} and f_{oc} , given ideal diodes. Diode voltage drop degrades output power (red curve) but the resulting 3-dB BW of 50 Hz (7.4% of f_{sc}) represents a substantial increase over a PEH with negligible coupling, where the 3-dB BW is $f_{sc}/Q_{ML}=17\text{Hz}$ (2.5% of f_{sc}).

Figure 5 shows the effect of varying κ_e^2 . These simulations show output power for PEHs having the CM parameters shown in Figure 2b, but with the parameter A varied to provide different κ_e^2 , where A represents the coupling between mechanical and electrical energy in a PEH. The simulations are made assuming a realistic 82% BF efficiency. They further assume the use of a smart switching rectifier in the DCRS/BF circuit of Figure 2c to eliminate the diode-voltage loss around f_{sc} . When κ_e^2 is small, maximum output power occurs at $f_{ZR1} \approx f_{sc}$. As κ_e^2 increases, the 3-dB BW increases. Use of the smart switching rectifier increases the BW with the present device ($\kappa_e^2=0.069$) to 78 Hz (11.5% of f_{sc}); if κ_e^2 can be increased by a factor of 2, the 3-dB BW increases to 104 Hz (15.4% of f_{sc}).

5. Design for Large κ_e^2

The coupling coefficient κ_e^2 is given by [9]

$$\kappa_e^2 = A^2 C_m / C_P = A^2 / (k C_P) = A^2 / ((k_{PE} + k_{non-PE}) C_P) = (f_{oc}^2 - f_{sc}^2) / f_{sc}^2 \quad (3)$$

where C_m represents the beam stiffness, C_P represents the plate capacitance of the piezoelectric material, k is the total spring constant of a PEH, k_{non-PE} and k_{PE} are spring constants of non-PE and PE component respectively. For the bimorph cantilever of Figure 1, A is given by [10]

$$A = 3WY_{PE}b_{PE}d_{31}/L \quad (4)$$

where W and L are width and length of a PEH, b_{PE} is the distance from the center-line of the cantilever to the center-line of the piezoelectric (PE) layer, Y_{PE} is the Youngs modulus of PE material, and d_{31} is the piezoelectric coefficient.

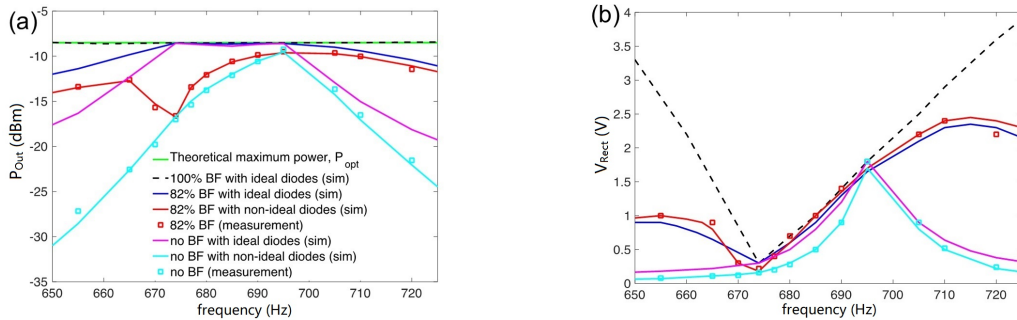


Figure 4. (a) Maximum output power and (b) corresponding value of V_{Rect} that gives maximum output power for a variety of load conditions.

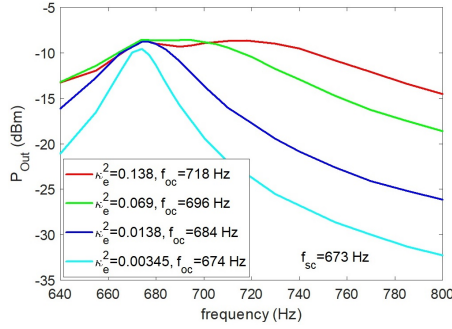


Figure 5. Output power for PEHs having different κ_e^2 .

A and C_P depend only on the PE material. It is apparent that k_{non-PE} should be made as small as possible. Thus, a composite cantilever designed for large κ_e^2 should be designed such that the electrodes and non-PE outer protection layers have low Young's modulus, and are as thin as possible. But the Young's modulus of non-PE material shouldn't be too small such that shearing occurs and two PE layers vibrate independently. Additionally, increasing the coupling term A also leads to a large κ_e^2 . If the PE material is predetermined in the design, increasing b_{PE} is a good choice to increase A. While changing of W or L is not suggested since not only A but also C_P and k are related to W and L. To increase b_{PE} , thick non-PE material should be inserted in between two PE layers, and the device center-line has minimal impact on spring constant.

Figure 6a shows the cross section of the commercial PPA2014. The non-PE material in this device contributes 41.6% of the total spring constant, and the κ_e^2 is calculated to be 0.053 (0.069 measured) with 5 mm clamping overlap. A redesigned device is shown in Figure 6b. The redesigned device retains the original L and W. To reduce k_{non-PE} , the Cu electrodes are removed, and the FR4 outer layer is replaced by polyimide which has a lower Young's modulus. Thicker PE capacitors are adopted to increase k_{PE} . In addition, a thicker center FR4 layer is used to increase b_{PE} so that A is increased. In the redesigned device, with a 5 mm clamping overlap, the non-PE material contributes 5.6% of the spring constant, and κ_e^2 is predicted to be increased by 2x to $\kappa_e^2=0.121$.

6. Conclusions

One factor that has prevented the widespread commercial use of PEHs is the narrow range of vibration frequencies over which (near) optimum power can be harvested. This paper shows that, with a combination of bias-flip electronics, smart rectification, and a PEH optimized for large κ_e^2 , one can achieve a fractional 3-dB BW in excess of 15%.

References

- [1] Guyomar D, Badel A, Lefeuvre E and Richard C 2005 *IEEE T. Ultrason. Ferroelectr. Freq. Control.* **52** 584
- [2] Ramadass Y and Chandrakasan A 2010 *IEEE J. SolidSt. Circ.* **45** 189
- [3] Zhao S, Ramadass Y, Lang J, Ma J and Buss D 2014 *Proc. IEEE S3S Conf.* 1
- [4] Lefeuvre E, Badel A, Richard C and Guyomar D 2005 *J. Intel. Mat. Syst. Str.* **16** 865
- [5] Wu W, Wickenheiser A, Reissman T and Garcia E 2009 *Smart Mater. Struct.* **18** 055012
- [6] Zhao S, Paidimarri A, Ickes N, Araghchini M, Lang J, Ma J, Ramadass Y and Buss D 2015 *Proc. IEEE S3S Conf.* 1
- [7] Hsieh P, Chen C and Chen H 2015 *IEEE. T. Power. Electr.* **30** 3142
- [8] Dutoit N, Wardle B and Kim S 2005 *Integr. Ferroelectr.* **71** 121
- [9] Shu Y and Lien I 2006 *Smart Mater. Struct.* **15** 1499
- [10] Erturk A and Inman D J 2009 *Smart Mater. Struct.* **18** 025009

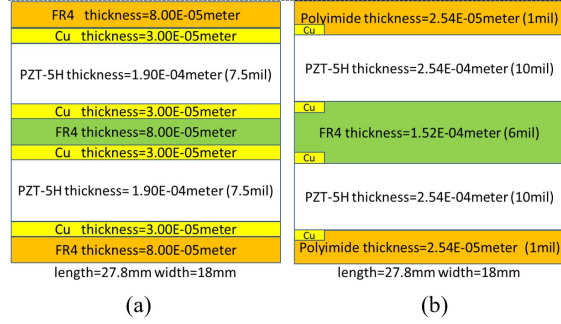


Figure 6. (a) Cross section of baseline device and (b) proposed redesign.